RSC Advances

REVIEW

Graphene-based photocatalytic composites

Xiaoqiang An and Jimmy C. Yu*

The use of graphene to enhance the efficiency of photocatalysts has attracted much attention. This is because of the unique optical and electrical properties of the two-dimensional (2-D) material. This review is focused on the recent significant advances in the fabrication and applications of graphene-based hybrid photocatalysts. The synthetic strategies for the composite semiconductor photocatalysts are described. The applications of the new materials in the degradation of pollutants, photocatalytic hydrogen evolution and antibacterial systems are presented. The challenges and opportunities for the future development of graphene-based photocatalysts are also discussed.

1. Introduction

Photocatalytic nanomaterials are attracting more and more attention because of their potential for solving environmental and energy problems, which are the biggest challenges of the 21st century.[1] Many research papers and review articles are dedicated to this topic.[2,3] Recently, the design and potential applications of nanostructured semiconductor materials for environment, energy and water disinfection have been reviewed by our group.[4,5] However, several fundamental issues must be addressed before the photocatalysts are economically viable for large scale industrial applications. For example, the fast recombination of electron–hole pairs and the mismatch between the band gap energy and solar radiation spectrum limit the applicability of TiO_2, which is considered as one of the best photocatalysts.[6]

As shown in Fig. 1, upon absorption of photons with energy larger than the band gap of a photocatalyst, electrons are excited from the valence band to the conduction band, creating electron–hole pairs. These charge carriers either recombine or migrate to the surface to initiate a series of photocatalytic reactions. The photocatalysis process usually involves several highly reactive species, such as $^{\bullet}OH$, $^{\bullet}O^{2-}$, and H_2O_2.

In order to improve the photocatalytic activities of photocatalysts, three key points should be addressed. They are: (1) the extension of excitation wavelength, (2) a decrease of charge carrier recombination, and (3) the promotion of active sites around the surface.[7,8] Attempts have been made and several strategies have been developed including: (1) doping with either anions or cations,[9,10] (2) surface coupling with metals or semiconductors,[11,12] and (3) improving the structure of photocatalysts in order to increase their surface area, porosity or reactive facets.[13–15] Fig. 2 shows the common types of 0-D, 1-D, 2-D and 3-D photocatalysts with enhanced photocatalytic

performance. Despite these developments, the commercial installation of photocatalytic systems for water splitting and chemical waste treatment is yet to be realized.[16]

Carbonaceous nanomaterials have unique structures and properties that can add attractive features to photocatalysts.[17,18] The coupling of carbon nanotubes (CNTs) to titanium dioxide has been reviewed by Sigmund and co-workers.[19] Generally, the photocatalytic enhancement is ascribed to the suppressed recombination of photogenerated electron–hole pairs, extended excitation wavelength and increased surface-adsorbed reactant, although the underlying mechanisms are still unclear. The recent progress in the development of TiO_2/nanocarbon photocatalysts has been reported by Westwood *et al.*, covering activated carbon, [60]-fullerenes, carbon nanotubes, graphene and other novel carbonaceous nanomaterials.[20]

As the most recently discovered carbonaceous material, graphene has attracted immense attention.[21,22] With a unique sp^2 hybrid carbon network, it shows great applications such as nanoelectronics, sensors, catalysts and energy conversion.[23–28] The application of graphene-based assemblies to boost the efficiency of solar energy conversion has been reviewed.[29–32]

Department of Chemistry and Institute of Environment, Energy and Sustainability, The Chinese University of Hong Kong, Shatin, New Territories, Hong Kong, China. E-mail: jimyu@cuhk.edu.hk; Fax: (+852)2603-5057; Tel: (+852)3943-6268
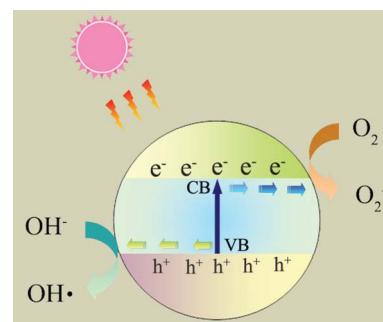

Fig. 1 Photoexcitation of a semiconductor and the subsequent generation of radicals or intermediate species, which are involved in the photocatalytic reaction.

This journal is © The Royal Society of Chemistry 2011
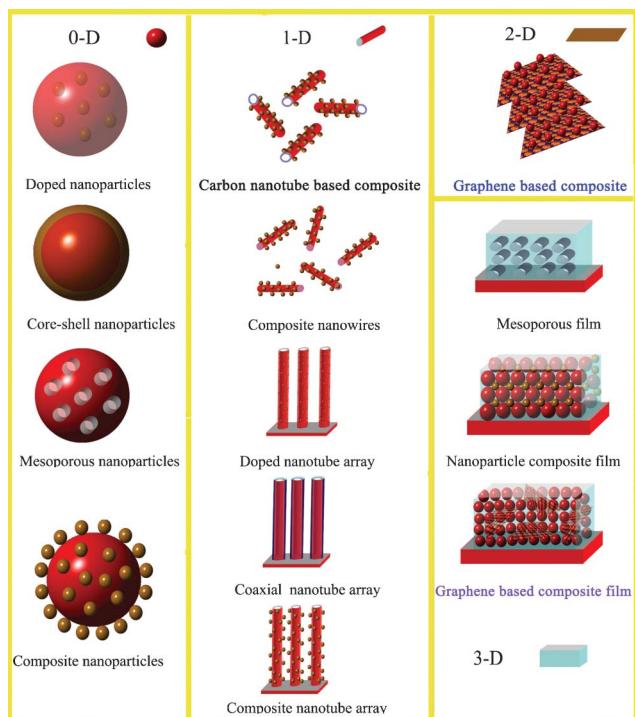
Fig. 2 Types of 0-D, 1-D, 2-D and 3-D photocatalysts with improved photocatalytic properties.

Graphene-based architectures are also highly desirable in the field of photocatalysis, for their promising energy and environmental applications.[33] Utilization of single-layer graphene sheets can not only provide a high quality 2-D photocatalyst support, but also a 2-D circuit board, with an attractive potential to harness their perfect electrical and redox properties. The field of graphene-enhanced photocatalysis is advancing fast, and a comprehensive review on the latest developments is greatly needed.

In this review, we will cover recent advances in the synthesis and photocatalytic applications of graphene-based nanoarchitectures. Particular attention will be paid to photodegradation of organic pollutants and the photocatalytic hydrogen evolution using TiO_2/graphene and ZnO/graphene photocatalysts. The major challenge and opportunity for future research will also be discussed. We hope this would be helpful for the design and fabrication of novel photocatalysts with greater performances.

2. Synthesis of graphene and graphene-based composites

Graphene is an exciting material, with a large theoretical specific surface area (2630 m^2 g^{-1}) and a high intrinsic electron mobility (200, 000 cm^2 V^{-1} s^{-1}).[34] Its optical transmittance ($\sim$97.7%) and good electrical conductivity merit attention for its application as a photocatalyst support.[35] At present, several methods have been developed to fabricate graphene, either through chemical or physical routes.[36–38] Although micromechanical exfoliation and chemical vapor deposition can produce high quality graphene for applications, their insufficient functional groups make the dispersion and contact with photocatalysts difficult.[39] However, the chemical oxidation of graphite to graphene oxide (GO) and
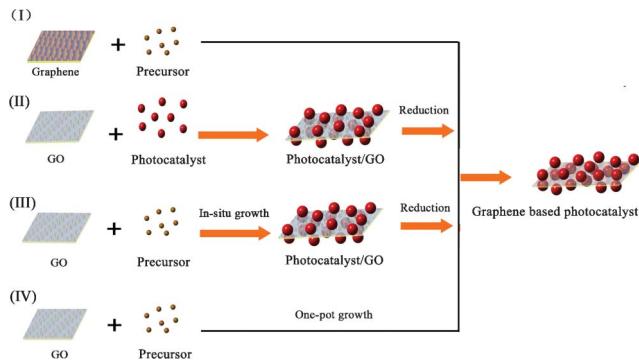

Fig. 3 Four synthetic strategies for the fabrication of graphene-based photocatalysts.

subsequent chemical reduction has been evaluated as one of the most efficient methods to fabricate graphene-based photocatalysts. The existence of carboxyl and epoxides makes graphene oxide suspendable in both polar and nonpolar solvents, which is essential for the uniform loading of the catalysts on the 2-D supports. Under the following reducing reaction, reduced graphene oxide (RGO) could partially restore the lost conductivity.[40] It is believed that the interactions between remaining carboxylic groups of RGO and the surface hydroxyl groups of photocatalysts strengthen their interactions.[41]

The synthetic strategies of graphene-based photocatalysts can be divided into four types, based on the formation sequence of the graphene and semiconductor photocatalysts.[42] The general strategies are shown in Fig. 3.

For method I, composite photocatalysts are fabricated by an *in situ* growth of photocatalysts on graphene sheets. It should be noted that pristine graphene usually has poor solubility in both polar and apolar solvents. Chemical modification is often necessary to avoid the aggregation of graphene sheets and to enhance their interactions with the photocatalysts. Recently, the instantaneous formation of metal oxide nanoparticles on graphene has been reported, under solvent-free microwave conditions.[43] The surface modification of graphene is an effective way to increase its compatibility and surface active sites.[44,45] Zhang *et al.* investigated the influence of electron beam pretreatment on the growth of TiO_2 clusters on graphene.[46] Carbon oxygen bands excited by electron beam irradiation on the graphene surface were considered as defect sites, which could increase the affinity of graphene to Ti^{4+} through an electrostatic force, thus providing more growth sites for TiO_2 crystals.

For method II, a photocatalyst with a well-defined structure is deposited on the surface of GO under vigorous stirring or ultrasonic agitation.[47] The site-specific oxygenated groups on GO facilitate the uniform distribution of photocatalysts. Graphene-based nanoarchitectures are obtained after the reduction of GO in the composite. For example, the cooperation of graphene with commercial TiO_2 nanopowders P25 (20% rutile and 80% anatase) has been researched. Several techniques can be applied to restore the sp^2 hybridization in GO, such as the hydrothermal reaction, thermal irradiation, the photocatalytic reaction or by the adoption of reductants (hydrazine, $NaBH_4$, *etc.*).[48–51] After the reduction of GO, either semiconductor/graphene hybrid powders or films with an enhanced photocatalytic property can be obtained.[52]

For the efficient electron transfer between graphene and nanoparticles, a homogeneous distribution of semiconductor nanoparticles on individual graphene is needed. This can be achieved by an *in situ* growth/reduction procedure or a simple one-pot growth method. In these strategies, the reduction of GO to graphene can be accomplished either in a subsequent reaction step (Method III),[53,54] or in an auto-redox reaction of the precursor (Method IV).[55] For instance, a TiO$_2$/GO composite was synthesized sonochemically from TiCl$_4$ and GO, and then reduced to TiO$_2$/RGO by the reaction with hydrazine.[56] In these processes, nanoparticles can also act as a stabilizer for avoiding the agglomeration of graphene.

As a convenient procedure, method IV shows its unique advantage for the fabrication of graphene-based photocatalysts. Usually, a redox reaction is needed to restore the conjugated structures of graphene. The reducing environment can be achieved through the utilization of reductive solvent or the addition of reductants directly.[57] For example, TiO$_2$/graphene composites were fabricated *via* a one-pot water-phase synthesis, using GO and TiCl$_3$ as the starting materials. TiCl$_3$ reduces GO to graphene while itself is hydrolyzed to another building block of the composite, titanium dioxide.[58] The utilization of low-valence metal salts is a facile and efficient strategy, both as the metal source and reductant for the restoration of graphene. The controlled nucleation is important to ensure the growth of nanoparticles on the surface of graphene. For example, SnO$_2$/graphene and TiO$_2$/graphene composites could be fabricated *via* a direct redox reaction between GO and the reactive cations Sn^{2+} and Ti^{3+}, as shown in Fig. 4. During the redox reaction, GO was reduced to RGO while Sn^{2+} and Ti^{3+} were oxidized to SnO$_2$ and TiO$_2$ and deposited on the surface of RGO.[59]

Several other novel methods have also been used to fabricate graphene-based nanoarchitectures. For instance, a self-assembly method was used to anchor TiO$_2$ nanorods on the surface of GO sheets.[60] After the carbonization of surface complexes between TiO$_2$ and 2,3-dihydroxynaphthalene, Kamegawa *et al.* fabricated graphene coated TiO$_2$ nanoparticles loaded on mesoporous

Fig. 4 One-pot synthesis of SnO$_2$/graphene and TiO$_2$/graphene photocatalysts. Reprinted from ref. 59.

silica.[61] The selective coating led to the enhancement of photocatalytic activities of TiO$_2$/MCM-41 for the decomposition of 2-propanol. Recently, a TiO$_2$/graphene composite has also been fabricated through the *in situ* growth of TiO$_2$ in the interlayer of expanded graphite under solvothermal conditions. The use of a vacuum-assisted technique and surfactant facilitated the distribution of TiO$_2$ and the exfoliation of expanded graphite.[62]

3. Graphene-based photocatalytic composites

3.1 TiO$_2$/graphene photocatalysts

Ever since the early development of photocatalytic technology in the 1970s, TiO$_2$ constitutes the dominating photocatalyst due to its high efficiency, low cost and good stability.[63] TiO$_2$/graphene composites with enhanced photocatalytic activities are currently being considered as one of the most promising candidates for photocatalytic applications.

Combination of P25 with graphene: The coupling of P25 with graphene has been widely researched, with an obvious enhancement of photocatalytic performance.[64] Chemically bonded P25/graphene nanocomposites have been fabricated through a one-step hydrothermal reaction, with *ca.* 1 wt% of graphene content. Because of the distribution of carboxylic acid groups on GO, P25 nanoparticles dispersed on the carbon support and had a tendency to accumulate along the wrinkles and edges. P25/graphene composites showed significant improvement in the photodegradation of methylene blue (MB) compared to P25, and they also exhibited higher efficiencies than P25/CNTs composites by *ca.* 20%.[65] In another research, Fan *et al.* fabricated P25-RGO composites by hydrazine reduction, UV-assisted photoreduction and a hydrothermal method. These P25/RGO composites showed different photocatalytic activities for H$_2$ evolution, in the order of P25-RGO-hydrothermal > P25-RGO photoreduction > P25-RGO-hydrazine. For comparison, a similar procedure was employed to prepare a P25-CNT composite. It was revealed that the P25-RGO composite is more effective than the P25-CNT composite for the evolution of H$_2$.[66] The differences between P25/CNTs and P25/graphene composite photocatalysts during the gas-phase degradation of benzene and liquid-phase degradation of dyes have also been investigated by Zhang and co-workers.[67] They suggested that TiO$_2$/graphene was in essence the same as other TiO$_2$/carbon (carbon nanotubes, fullerenes, and activated carbon) composite materials on improving the photocatalytic activity of TiO$_2$.[68]

These conflicting results indicate the complexity of graphene-based photocatalysts. After all, the integrated photocatalytic property of graphene-based composites is influenced by several factors, such as the electrical property of graphene, the interfacial contact and charge transfer between graphene and nanoparticles. As to the RGO with a partial restored sp^2 structure, the lost conductivity caused by the defects should also be mentioned.[69] The coupling of photocatalysts to high-quality graphene is challenging but desirable.[70] The unique 2-D structure of graphene sheets benefits the efficient anchoring of semiconductor photocatalysts on their surface.[71] To a certain extent, the improved interfacial contact makes it a better choice for catalytic support.[72]

Growth of TiO$_2$ on graphene: In order to fabricate high-efficiency photocatalysts, many groups are devoted to the growth
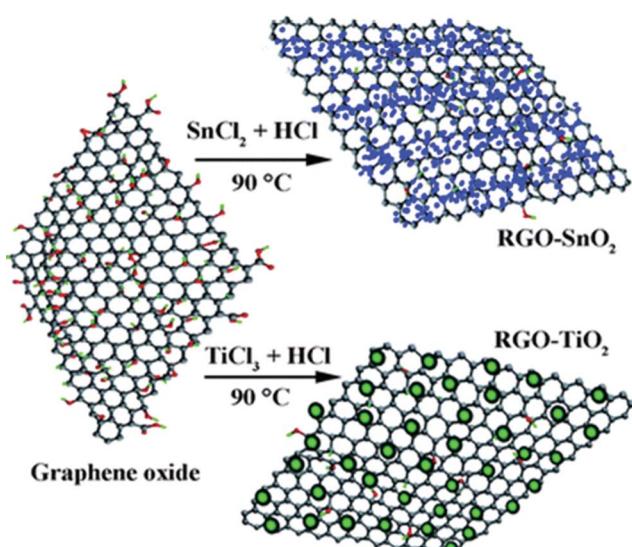
of TiO_2 nanostructures on graphene through *in situ* or one-pot routes.[73] The effects of a uniform coating and strong coupling between TiO_2 and GO on the degradation of rhodamine B (RhB) have been studied by Liang and co-workers. The apparent rate constant of simple P25/graphene mixture ($k = 0.09$ min^{-1}) was less than half that of the *in situ* TiO_2/graphene hybrid photocatalysts (0.2 min^{-1}).[74] Chen *et al.* investigated the influence of interfacial stress on the property of TiO_2/GO composites. They found that the formation of a p-type and n-type semiconductor could be tuned through the concentration of TiO_2. When GO formed a p-type semiconductor, a p/n heterojunction could be clearly observed. Photocatalytic activity tests showed that the semiconductors formed by GO on the surface of photocatalysts could act as a sensitizer and enhance their visible-light photocatalytic performance.[75] The influence of graphene content and calcination atmosphere on the photocatalytic activities has also been researched. Better performance than that of P25 for H_2 evolution was demonstrated for the TiO_2/graphene composites and the highest activity was observed for the sample with 5% graphene. The samples calcined in a nitrogen atmosphere showed higher activities than those calcined in air.[76]

TiO$_2$/graphene composite films: Photocatalytic films are among the best candidates for photocatalytic applications, because of their features of easily fixing, recycling and restoring. Enhanced efficiency of the photodegradation was found after coating TiO_2 films with GO.[77] It was related to the efficient charge separation and transportation among the giant π-conjugation and planar structure. Du and co-workers coupled hierarchically ordered macro-mesoporous titania films to graphene, through a confined self-assembly method.[78] The SEM and TEM images of macro-mesoporous titania films are shown in Fig. 5. It was found that the existence of interconnected macropores in mesoporous films significantly improved the mass transport through the film, reduced the length of the mesopore channel, and increased the accessible surface area within the thin film. The apparent rate constants for macro-mesoporous films without and with graphene were about 11 and 17 times higher than that of pure mesoporous titania films.

3.2 Metal oxide/graphene and metal sulfide/graphene photocatalysts

Many non-TiO_2-based photocatalysts have been fabricated.[79] It has been reported that many metal oxide compounds showed similar photocatalytic capabilities, such as ZnO, SnO_2, WO_3, Fe_2O_3 *etc.*[80] Among these, ZnO is often considered as a favorable alternative to TiO_2 for photocatalytic applications. The *in situ* growth method has been used to combine ZnO nanoparticles with GO, which could be converted into ZnO/graphene nanoarchitectures after chemical reduction.[81] With 2 wt% graphene content, Xu *et al.* achieved 4 times' enhancement of photocatalytic activity, compared to that of pristine ZnO.[82] The *in situ* growth of Fe_3O_4 on graphene has also been reported, using sodium acrylate as a stabilizer in a one-pot reaction.[83] Taking the combined advantages of graphene and magnetic nanoparticles, these nanocomposites exhibited an excellent removal efficiency and a rapid separation from aqueous solution by an external magnetic field.

A ZnS/graphene nanocomposite with an excellent photocatalytic activity has been fabricated by a microwave irradiation method.[84] Thioacetamide was used as a sulfur source as well as a reducing agent. Recently, the decoration of graphene with a familiar visible-light-driven photocatalyst has been reported. The optimal weight percentage of graphene in the CdS clusters/graphene nanocomposites was found to be 1.0 wt%, which resulted in a high photocatalytic H_2-production rate of 1.12 mmol h^{-1}. The corresponding apparent quantum efficiency approached 22.5% at 420 nm.[85]

3.3 Metallate/graphene photocatalysts

Recently, interest has been dedicated to the photocatalytic applications of metallates, one type of more complex oxides.[86] The combination of $BiWO_6$ with graphene has attracted a lot of attention, as it is considered as the most important visible-light-driven photocatalyst among the Bi^{3+}-based oxides.[87] The electronic interaction and charge equilibration between graphene and Bi_2WO_6 led to the shift of the Fermi level and decreased the conduction band potential. The enhanced photocatalytic activity of $BiWO_6$/graphene nanoarchitectures was ascribed to the negative shift in the Fermi level and the high migration efficiency of photoinduced electrons.[88] During the photoelectrochemical water splitting reaction, a remarkable 10-fold enhancement was observed after the incorporation of $BiVO_4$ with graphene.[89] Similarly, the photocatalytic performance of γ-Bi_2MoO_6 has also been improved by 4 times after their cooperation with 1% graphene.[90]

Lately, Fu and co-workers prepared a magnetically separable $ZnFe_2O_4$/graphene nanocomposite photocatalyst. The photocatalyst exhibits dual functions as a photoelectrochemical degrader and a generator of hydroxyl radicals *via* photoelectrochemical decomposition of H_2O_2.[91] Zhang *et al.* reported the photocatalytic activities of $InNbO_4$/graphene nanocomposites. The kinetic constants of MB and 2,4-dichlorophenol removal with $InNbO_4$/graphene were respectively 1.87 and 2.1 times than with $InNbO_4$.[92]
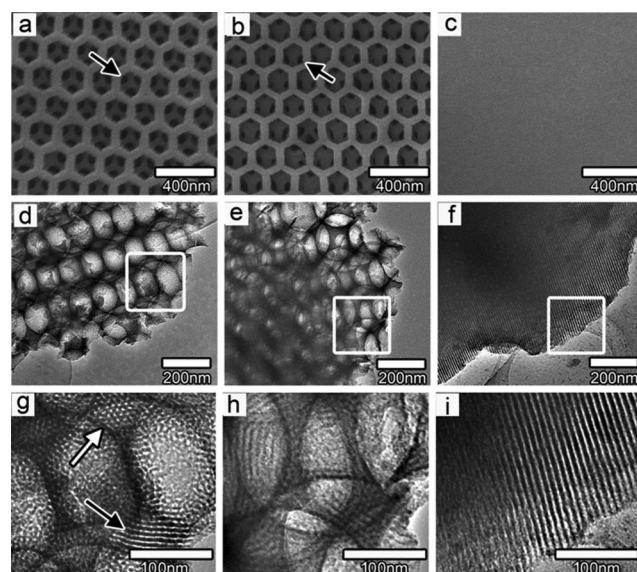

Fig. 5 Typical SEM and TEM micrographs of macro-mesoporous titania films (a, d, g) without and (b, e, h) with graphene and pure mesoporous titania film (c, f, i). Reprinted with permission from ref. 78. Copyright 2010 American Chemical Society.

3.4 Other graphene-based photocatalysts

The coupling of graphene to several other nanomaterials has also been explored. Zhu and co-workers fabricated visible-light-driven plasmonic photocatalysts based on Ag/AgX (X = Br, Cl)/GO nanocomposites, achieving enhanced photocatalytic activity and excellent stability.[93] In another research, GO and RGO were pillared with CNTs by using acetonitrile as a carbon source in the chemical vapor deposition method. The unique porous structure and the exceptional electron transfer property resulted in the excellent visible-light activity of the CNT-pillared RGO composite.[94] Xiong *et al.* investigated the effect of modification of RGO with crystalline copper species. The copper species acted as an electron relay, passing the excited electrons from the RGO to the adsorbed oxygen. The continuously generated reactive oxygen species led to the degradation of RhB under visible-light irradiation.[95]

4. Application of graphene-based photocatalysts

Photocatalysts are expected to play an important role in solving many serious environmental and pollution challenges.[96–99] As shown in Fig. 6, graphene-based photocatalysts mainly show significant photocatalytic applications in three fields: (1) degradation of organic pollutants into more environmentally friendly chemical species; (2) photocatalytic hydrogen generation where solar energy is converted into a hydrogen fuel; and (3) photocatalytic conversion of CO_2 to hydrocarbon fuels.[100,101]

4.1 Photodegradation of organic compounds and the mechanism

After photoexcitation, several types of radicals or intermediate species are generated. Among them, hydroxyl radicals are a powerful oxidizing agent able to attack the molecules around the surface of photocatalysts.[102] The application of the photocatalysts in the destruction of both organic and inorganic compounds has been widely investigated.[103] Table 1 shows the recent reports on the photodegradation of organic compounds by using graphene-based photocatalysts.

Recently, the photodegradation of cationic dye MB with graphene-based composites has been studied. The photocatalytic activity of TiO_2/graphene composite is significantly enhanced under both ultraviolet and visible light irradiation. Several methods have been adopted to clarify the possible photocatalytic mechanism for the enhancements. Liu and co-workers fabricated RGO wrapped TiO_2 hybrid by one-step photocatalytic reduction. They demonstrated that RGO captured dyes and photo-induced electrons during the photocatalytic degradation of organic dyes in water.[104] Wang *et al.* investigated the photo-induced charge transfer between TiO_2 and graphene, using a transient photovoltage technique.[105] After their integration with graphene, the mean life time of electron–hole pairs was prolonged from $\sim 10^{-7}$ s to $\sim 10^{-5}$ s. Thus, dual roles of graphene in the composite were improved by: (1) increasing the electron–hole pair separation through the electron injection from conduction band of TiO_2 into graphene, (2) greatly retarding the recombination of electron–hole pairs in the excited TiO_2.

High photocatalytic activities were observed when graphene-based composites were used in the photodegradation of RhB. Direct electron transfer from RhB* to the graphene semiconductor was found to be thermodynamically favorable and much more feasible than to TiO_2. In Fig. 7, different electron transfer pathways and photosensitization process were used to explain the different photocatalytic activities of SnO_2 and TiO_2.[59] Because of the efficient injection of electron from excited RhB to graphene, it was believed that graphene acted as an electron mediator to facilitate the electron transfer from RhB* to SnO_2. But for those RhB adsorbed on the surface of TiO_2, the excited RhB* could directly inject electrons into the TiO_2, and the electrons could continuously move to the graphene sheet or be trapped by the molecular oxygen. The similar electron transfer from RhB* to graphene and subsequent move was also used to illustrate the possible mechanism of the Au/graphene composite photocatalyst.[106] This spatially separated RhB+ and electrons, thus retarded the recombination process and improved their photocatalytic performance.

Graphene-based photocatalysts also show promising applications in the degradation of other organic molecules. Ng *et al.* fabricated homogeneous TiO_2/graphene thin film through the deposition of TiO_2/graphene suspension. During the degradation of 2,4-dichlorophenoxyacetic acid with TiO_2/graphene films, a 4-fold increase in the rate of photocatalytic degradation was
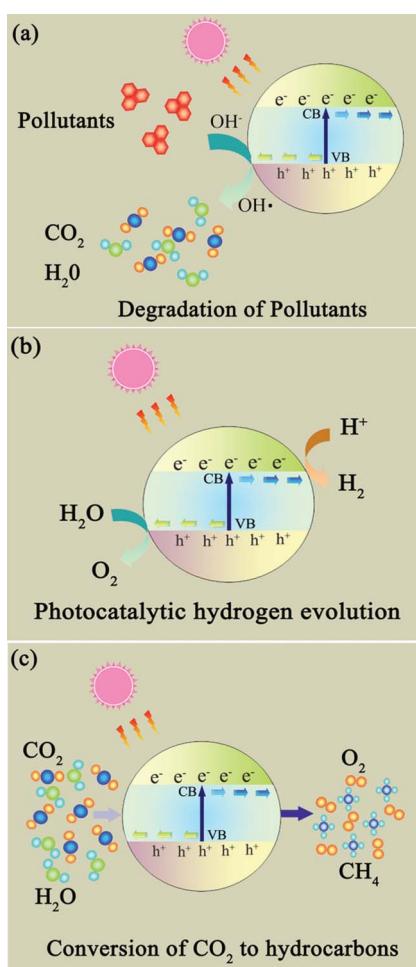

Fig. 6 The photocatalytic applications of photocatalysts. (a) Degradation of organic pollutants; (b) photocatalytic hydrogen generation; (c) photocatalytic conversion of CO_2 to hydrocarbon fuels.

Table 1 Recent reports on the use of graphene-based photocatalysts for degrading selected organic pollutants

Type of catalysts	Graphene content	Pollutants	Results	Reference
P25/Graphene	1%	Methylene blue	20% higher than P25-CNTs	65
P25/Graphene oxide	8.2 wt(%)	Methylene blue	Apparent rate constant increased by a factor of 8.52 than P25	108
P25/Graphene	10%	Methylene blue	70% degraded after 5h, compared to 10% of P25.	64
P25/Graphene	0.50%	Benzene	Conversion maintained at 6.4%. For P25 it decreased from 5.8% to 1.2% after 28 h.	67
P25/Graphene	5%	Methylene blue	GR was in essence the same as CNT.	67
TiO_2/Graphene	15 wt(%)	Rhodamine B	Rate constant of SnO_2 and TiO_2 is 2.2 and 1.2 times higher than P25.	59
TiO_2/Graphene	75%	Methylene blue	The k value was 2.5 times higher than P25.	56
TiO_2/Graphene	30 mg	Methylene blue	75% in 3 h, improved compared to P25.	52
TiO_2/Graphene	—	Methyl orange	Much higher than P25/Graphene.	46
TiO_2/Graphene Oxide	0.14%	Methyl orange	Higher than P25.	75
TiO_2/Graphene	10 wt(%)	Rhodamine B	Apparent rate constant was three times higher than P25.	74
TiO_2/Graphene oxide	4.60%	Methyl orange	The photo-oxidative degradation rate of methylorange was as high as 7.4 times that over P25.	120
Graphene/TiO_2/MCM-41	0.15 wt(%)	2-propanol	Photocatalytic activity was enhanced after graphene coating.	61
TiO_2 nanorods/Graphene oxide	40% TiO_2	C.I. Acid Orange	TiO_2 nanorods show higher efficiency than that of TiO_2 nanoparticles	126
TiO_2 nanorods/Graphene oxide	30%	Methylene blue	Significant increase was achieved compared to P25.	60
TiO_2/Graphene Oxide film	0.03 mg	Methylene blue	TiO_2/Graphene oxide showed improvement compared to TiO_2 film.	77
TiO_2/Graphene film	—	2,4-dichlorophenoxy-acetic acid	Rate constant was four times higher than TiO_2 film.	107
Macro-Mesoporous TiO_2/Graphene	0.6 wt(%)	Methylene blue	Apparent rate constant was 1.6 times higher than Macro-Mesoporous TiO_2.	78
ZnO/Graphene	—	Rhodamine B	The degradation rate was remarkably enhanced.	81
ZnO/Graphene	2 wt(%)	Methylene blue	The activity was increased by almost four times than ZnO.	82
ZnS/Graphene	—	Methylene blue	ZnS/graphene had a more excellent photocatalytic activity.	84
Fe_3O_4/Graphene	—	Rhodamine B, malachite green	91% rhodamine B and 94% malachite green were removed.	83
Au/Graphene	—	Rhodamine B	Rate constant was 1.8 times than P25.	106
Bi_2WO_6/Graphene	—	Rhodamine B	The activity was 3 times greater than that of the Bi_2WO_6 sample.	88
γ-Bi_2MoO_6/Graphene	1 wt(%)	Methylene blue	The activity increased by 4 times after 1.0 wt% of graphene loaded.	90
$ZnFe_2O_4$/Graphene	20 wt(%)	Methylene blue	The activity was enhanced after the addition of H_2O_2, 88% MB was degraded in 5 min.	91
$InNbO_4$/Graphene	3 wt(%)	Methylene blue	The kinetic constant was 1.87 times greater than that with $InNbO_4$.	92
CNTs/Graphene	—	Rhodamine B	4 times faster than that of P25	94
Cu modified graphene	10 wt(%)	Rhodamine B	3 times faster than that of P25	95

achieved.[107] Photocatalytic degradation of the anionic surfactant dodecylbenzenesulfonate (DBS) has been reported, using Pt/graphene/TiO_2 nanocomposites. The mineralization of DBS was enhanced by a factor of 3, compared to that of P25.[109]

Based on the above results, the enhanced photocatalytic degradation of organic compound could be attributed to the following reasons: (1) the interactions between organic molecules and the aromatic regions of graphene enhance the adsorption on photocatalysts.[110] (2) the formation of the Ti–O–C chemical bond narrows the band gap of TiO_2 and extends the photoresponding

range.[111] (3) the transfer of excited electrons from TiO_2 to graphene suppresses the charge recombination.[112,113]

4.2 Hydrogen evolution from water photocatalytic splitting

Hydrogen evolution from photocatalytic water splitting is an attractive process because it is a renewable energy production with no reliance on fossil fuels and no carbon dioxide emission.[114] During this process, the inhibited recombination of photoinduced carriers and the extended light absorption are important considerations. Graphene oxide is an intermediate state between graphene and graphite, the promising application of this p-doped material for the evolution of H_2 from splitting water has been reported.[115] Through controlling the oxidation level, their electronic properties could be tuned. As a result, GO with moderate oxidation level steadily catalyzed H_2 generation from a 20 vol% aqueous methanol solution under irradiation with UV or visible light.

Because of the superior electrical property of graphene, there is a great interest in combining photocatalysts with graphene to improve their conductivity and H_2 production activity. For example, TiO_2/RGO composites fabricated through ionic liquid-assisted hydrothermal method exhibited a hydrogen evolution rate of 20 μmol h^{-1}. That value was much better than the as-prepared TiO_2 nanoparticles and the TiO_2/CNT composites.[116] Metal-free graphite carbon nitride is considered as a promising visible-light-driven photocatalyst for water splitting. Lately, the
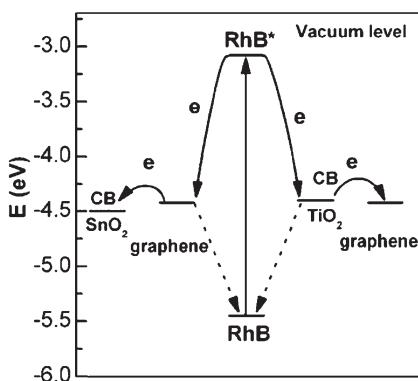

Fig. 7 The energy diagrams of RhB, graphene, TiO_2 and SnO_2. Reprinted from ref. 59.

combination of this polymeric photocatalyst with graphene has also been reported.[117] With an optimal graphene content of 1.0 wt%, the visible light H_2 production rate was increased to 451 μmol h^{-1} g^{-1}, which exceeded that of pure g-C_3N_4 by more than 3.07 times.

4.3 Other applications of graphene-based photocatalysts

Graphene enhanced photocatalysts are useful in environmental remediation, solar energy conversion, chemical synthesis, CO_2 reduction and antibacterial applications.[118]

Lately, Liang and co-workers investigated the influence of structural defects of graphene on the photocatalytic reduction of CO_2 for solar fuel production. Graphene with different defect densities was fabricated by two major solution-based pathways, oxidation–reduction and solvent exfoliation. P25/graphene nanocomposites based on the less defective solvent-exfoliated graphene exhibited a significantly larger enhancement in CO_2 photoreduction.[119] It was reported that TiO_2 nanoparticles assembled on GO nanosheets showed high photocatalytic activity for the photo-reductive conversion of Cr(VI). The conversion rate over the composites was as high as 5.4 times that over P25.[120] Akhavan et al. investigated the influence of a graphene coating on the antibacterial activity of the TiO_2 thin film.[121] Used as photocatalysts for the deactivation of E. coli bacteria in an aqueous solution, the photocatalytic reduction of GO platelets for 4 h caused an improvement of the antibacterial activity by a factor of about 7.5.

Interestingly, the photocatalytically generated highly reactive OH radicals can work as sharp chemical scissors for photocatalytic engineering of graphene for electronics.[122] Using a patterned TiO_2 photomask, Zhang et al. achieved various photochemical tailorings of graphene, including ribbon cutting, arbitrary patterning on any substrate and layer-by-layer thinning.[123] The patterned graphene was further used to fabricate all-carbon field effect transistor arrays.

5. Conclusions and perspectives

Coupling graphene with suitable semiconductor and metal nanostructures allows the design of next generation photocatalyst systems. In this review, we have summarized the recent advances in the fabrication and application of the new composite materials. These exciting developments have opened up new pathways to high-performance photocatalysts.

Despite the advances, great opportunities still exist in the exploitation of novel graphene-based hybrid assemblies. After all, the promotion of charge collection and transport by graphene may not be the exclusive pathway for enhanced photocatalytic activity in this synergistic system. The most common systems reported in the literature are based on the dispersion of semiconductor nanoparticles on the surface of graphene. As we know, the properties of photocatalysts are highly dependent on the surface structure of materials. Thus, the structural evolution of loaded nanomaterials on the 2-D supports should be highlighted, through controlling their morphologies, phase structures, porosities, surface active sites etc.[124,125] This has been demonstrated in recent reports on novel graphene-based photocatalysts. The influence of the morphology of TiO_2 on photocatalytic activity has been studied by Liu

et al.[126] The as-synthesized TiO_2 nanorod/graphene oxide composite showed much higher efficiency in the photocatalytic degradation of C. I. Acid Orange 7 and higher antibacterial activity than that of TiO_2 nanoparticle/graphene oxide. The high activity of TiO_2 nanorod/graphene oxide was found to be related to the abundance of (101) facets. Several other strategies have also been used for the structural optimization of photocatalytic nanoparticles on graphene, such as doping with nonmetals and coupling with metals. For example, increased photocatalytic hydrogen production was observed for a nitrogen doped and Pt coupled $Sr_2Ta_2O_7$/graphene photocatalyst.[127] Fig. 8 shows some other reported graphene-based nanoarchitectures, such as the distribution of TiO_2 nanorods, TiO_2 nanospindles and mesoporous TiO_2 nanoparticles on graphene nanosheets.[128–130] Further improvement of photocatalytic performance is expected via structural optimization of the graphene-based nanoarchitectures.

Moreover, the underlying mechanism of the photocatalytic enhancement by graphene-based nanoassembly is not fully understood. Generally, this enhancement is ascribed to the extended absorption and improved charge transfer in the hybrids.[131] To clarify the possible mechanism of photocatalytic reaction, research on the interfacial status of photocatalysts is important. Thus, many recent studies are devoted to understanding the structural changes and the manner of charge transfer around the surface of semiconductor and graphene. Lately, the density functional calculation method has been used to study the interface between graphene and rutile TiO_2. A significant charge transfer from graphene to titania was afforded, which resulted in the hole doping in graphene.[132] Thus, electrons in the upper valence band could be directly excited from graphene to the conduction band of titania under visible light irradiation, as that happened in TiO_2/CNT
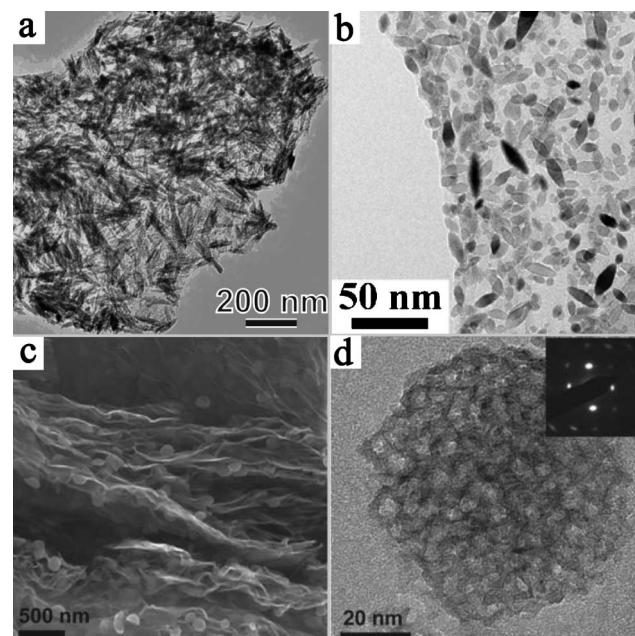
Fig. 8 Several types of TiO_2 nanostructures on graphene. (a) Rutile TiO_2/graphene. Reprinted with permission from ref. 128. Copyright 2010 American Chemical Society; (b) TiO_2 nanospindles/graphene oxide. Reprinted with permission from ref. 129. Copyright 2010 American Chemical Society; (c) and (d) mesoporous anatase TiO_2/graphene. Reprinted from ref. 130 with permission by Wiley-VCH.

hybrids.[19] This new role of graphene as the sensitizer to TiO_2 indicates that the graphene-based nanoarchitectures are more complex than expected.

Finally, the structural aspect of graphene sheets in the composites should not be overlooked, because of its tunable optical and electronic properties.[133] The fabrication of high-quality graphene-based composites is very challenging due to the existence of defects or oxidation sites in the partial-restored graphene.[134] More efficient synthetic strategies for graphene-based composites would need to be developed to address these issues.[135]

Acknowledgements

References

1 F. E. Osterloh, *Chem. Mater.*, 2008, **20**, 35.
2 K. Maeda and K. Domen, *J. Phys. Chem. Lett.*, 2010, **1**, 2655.
3 S. C. Roy, O. K. Varghese, M. Paulose and C. A. Grimes, *ACS Nano*, 2010, **4**, 1259.
4 X. Hu, G. Li and J. C. Yu, *Langmuir*, 2010, **26**, 3031.
5 D. Zhang, G. Li and J. C. Yu, *J. Mater. Chem.*, 2010, **20**, 4529.
6 X. Chen and S. S. Mao, *Chem. Rev.*, 2007, **107**, 2891.
7 X. Chen, S. Shen, L. Guo and S. S. Mao, *Chem. Rev.*, 2010, **110**, 6503.
8 T. Tachikawa, M. Fujitsuka and T. Majima, *J. Phys. Chem. C*, 2007, **111**, 5259.
9 Y. Huang, W. K. Ho, S. C. Lee, L. Z. Zhang, G. S. Li and J. C. Yu, *Langmuir*, 2008, **24**, 3510.
10 X. F. Yang, J. Chen, L. Gong, M. M. Wu and J. C. Yu, *J. Am. Chem. Soc.*, 2009, **131**, 12048.
11 S. Shanmugam, A. Gabashvili, D. S. Jacob, J. C. Yu and A. Gedanken, *Chem. Mater.*, 2006, **18**, 2275.
12 X. C. Wang, J. C. Yu, C. M. Ho and A. C. Mak, *Chem. Commun.*, 2005, 2262.
13 H. J. Wang, F. Q. Sun, Y. Zhang, L. S. Li, H. Y. Chen, Q. S. Wu and J. C. Yu, *J. Mater. Chem.*, 2010, **20**, 5641.
14 G. S. Li, D. Q. Zhang and J. C.Yu, *Chem. Mater.*, 2008, **20**, 3983.
15 C. L. Yu, J. C. Yu, W. Q. Zhou and K. Yang, *Catal. Lett.*, 2010, **140**, 172.
16 M. Kitano, M. Matsuok, M. Ueshima and M. Anpo, *Appl. Catal., A*, 2007, **325**, 1.
17 Y. Yu, J. C. Yu, J. Yu, Y. Kwok, Y. Che, J. Zhao, L. Ding, W. Ge and P. Wong, *Appl. Catal., A*, 2005, **289**, 186.
18 D. Eder, *Chem. Rev.*, 2010, **110**, 1348.
19 K. Woan, G. Pyrgiotakis and W. Sigmund, *Adv. Mater.*, 2009, **21**, 2233.
20 R. Leary and A. Westwood, *Carbon*, 2011, **49**, 741.
21 K. S. Novoselov, A. K. Geim, S. V. Morozov, D. Jiang, Y. Zhang, S. V. Dubonos, I. V. Grigorieva and A. A. Firsov, *Science*, 2004, **306**, 666.
22 Jeffrey Pyun, *Angew. Chem., Int. Ed.*, 2011, **50**, 46.
23 D. Wei and Y. Liu, *Adv. Mater.*, 2010, **22**, 3225.
24 M. J. Allen, V. C. Tung and R. B. Kaner, *Chem. Rev.*, 2010, **110**, 132.
25 J. S. Chen, Z. Wang, X. Dong, P. Chen and X. W. Lou, *Nanoscale*, 2011, **3**, 2158.
26 J. Yi, J. Lee and W. Park, *Sens. Actuators, B*, 2011, **155**, 264.
27 Y. Fan, H. Lu, J. Liu, C. Yang, Q. Jing, Y. Zhang, X. Yang and K. Huang, *Colloids Surf., B*, 2011, **83**, 78.
28 J. Johnson, A. Behnam, S. J. Pearton and A. Ural, *Adv. Mater.*, 2010, **22**, 4877.
29 P. V. Kamat, *J. Phys. Chem. Lett.*, 2011, **2**, 242.
30 Y. Hu, H. Wang and B. Hu, *Chem. Sus. Chem.*, 2010, **3**, 782.
31 H. Zhu, J. Wei, K. Wang and D. Wu, *Sol. Energy Mater. Sol. Cells*, 2009, **93**, 1461.
32 Y. Sun, Q. Wu and G. Shi, *Energy Environ. Sci.*, 2011, **4**, 1113.
33 K. Krishnamoorthy, R. Mohan and S. Kim, *Appl. Phys. Lett.*, 2011, **98**, 244101.
34 S. Guo and S. Dong, *Chem. Soc. Rev.*, 2011, **40**, 2644.
35 Y. Zhu, S. Murali, W. Cai, X. Li, J. Suk, J. R. Potts and R. S. Ruoff, *Adv. Mater.*, 2010, **22**, 3906.
36 M. Inagaki, Y. A. Kima and M. Endo, *J. Mater. Chem.*, 2011, **21**, 3280.
37 X. Jia, J. Campos-Delgado, M. Terrones, V. Meuniere and M. S. Dresselhaus, *Nanoscale*, 2011, **3**, 86.
38 M. Pumera, *Chem. Soc. Rev.*, 2010, **39**, 4146.
39 X. Cui, C. Zhang, R. Hao and Y. Hou, *Nanoscale*, 2011, **3**, 2118.
40 O. C. Compton and S. T. Nguyen, *Small*, 2011, **6**, 711.
41 G. Eda and M. Chhowalla, *Adv. Mater.*, 2010, **22**, 2392.
42 H. Bai, C. Li and G. Shi, *Adv. Mater.*, 2011, **23**, 1089.
43 Y. Lin, D. W. Baggett, J. Kim, E. J. Siochi and J. W. Connell, *ACS Appl. Mater. Interfaces*, 2011, **3**, 1652.
44 Y. Tang, C. Lee, J. Xu, Z. Liu, Z. Chen, Z. He, Y. Cao, G. Yuan, H. Song, L. Chen, L. Luo, H. Cheng, W. Zhang, I. Bello and S. Lee, *ACS Nano*, 2010, **4**, 3482.
45 C. N. R. Rao, A. K. Sood, K. S. Subrahmanyam and A. Govindaraj, *Angew. Chem., Int. Ed.*, 2009, **48**, 7752.
46 H. Zhang, P. Xu, G. Du, Z. Chen, K. Oh, D. Pan and Z. Jiao, *Nano Res.*, 2011, **4**, 274.
47 Z. Qiong, H. Y. Qiu, C. Gang, H. Hu, L. Jiang, Y. Ting and J. Li, *Chin. Sci. Bull.*, 2011, **56**, 331.
48 G. Williams, B. Seger and P. V. Kamat, *ACS Nano*, 2008, **2**, 1487.
49 O. Akhavan, *ACS Nano*, 2010, **4**, 4174.
50 O. Akhavan, *Carbon*, 2011, **49**, 11.
51 T. Wu, S. Liu, Y. Luo, W. Lu, L. Wang and X. Sun, *Nanoscale*, 2011, **3**, 2142.
52 Y. H. Ng, A. Iwase, N. J. Bell, A. Kudob and R. Amala, *Catal. Today*, 2011, **164**, 353.
53 B. Li, H. Cao, J. Shao, M. Qu and J. H. Warner, *J. Mater. Chem.*, 2011, **21**, 5069.
54 D. R. Dreyer, S. Park, C. W. Bielawski and R. S. Ruoff, *Chem. Soc. Rev.*, 2010, **39**, 228.
55 J. Shen, B. Yan, M. Shi, H. Ma, N. Li and M. Ye, *J. Mater. Chem.*, 2011, **21**, 3415.
56 J. Guo, S. Zhu, Z. Chen, Y. Li, Z. Yu, Q. Liu, J. Li, C. Feng and D. Zhang, *Ultrason. Sonochem.*, 2011, **18**, 1082.
57 J. Wu, X. Shen, L. Jiang, K. Wang and K. Chen, *Appl. Surf. Sci.*, 2010, **256**, 2826.
58 C. Zhu, S. Guo, P. Wang, L. Xing, Y. Fang, Y. Zhai and S. Dong, *Chem. Commun.*, 2010, **46**, 7148.
59 J. Zhang, Z. Xiong and X. S. Zhao, *J. Mater. Chem.*, 2011, **21**, 3634.
60 J. Liu, H. Bai, Y. Wang, Z. Liu, X. Zhang and D. Sun, *Adv. Funct. Mater.*, 2010, **20**, 4175.
61 T. Kamegawa, D. Yamahana and H. Yamashita, *J. Phys. Chem. C*, 2010, **114**, 15049.
62 B. Jiang, C. Tian, W. Zhou, J. Wang, Y. Xie, Q. Pan, Z. Ren, Y. Dong, D. Fu, J. Han and H. Fu, *Chem.–Eur. J.*, 2011, **17**, 8379.
63 M. D. Hernandez-Alonso, F. Fresno, S. Suarez and J. M. Coronado, *Energy Environ. Sci.*, 2009, **2**, 1231.
64 Y. Zhang and C. Pan, *J. Mater. Sci.*, 2011, **46**, 2622.
65 H. Zhang, X. Lv, Y. Li, Y. Wang and J. Li, *ACS Nano*, 2010, **4**, 380.
66 W. Fan, Q. Lai, Q. Zhang and Y. Wang, *J. Phys. Chem. C*, 2011, **115**, 10694.
67 Y. Zhang, Z. Tang, X. Fu and Y. Xu, *ACS Nano*, 2010, **4**, 7303.
68 L. Huang, B. Wu, G. Yu and Y. Liu, *J. Mater. Chem.*, 2011, **21**, 919.
69 S. Park and R. S. Rruoff, *Nat. Nanotechnol.*, 2009, **4**, 217.
70 X. Yan and L. Li, *J. Mater. Chem.*, 2011, **21**, 3295.
71 P. V. Kamat, *J. Phys. Chem. Lett.*, 2010, **1**, 520.
72 R. Mas-Balleste, C. Gomez-Navarro, J. Gomez-Herrero and F. Zamora, *Nanoscale*, 2011, **3**, 20.
73 K. Zhou, Y. Zhu, X. Yang, X. Jiang and C. Li, *New J. Chem.*, 2011, **35**, 353.
74 Y. Liang, H. Wang, H. S.Casalongue, Z. Chen and H. Dai, *Nano Res.*, 2010, **3**, 701.
75 Y. Chen, W. Cai, M. Long, B. Zhou, Y. Wu, D. Wu and Y. Feng, *ACS Nano*, 2010, **4**, 6425.
76 X. Zhang, H. Li, X. Cui and Y. Lin, *J. Mater. Chem.*, 2010, **20**, 2801.

77 D. Yoo, T. V. Cuong, V. H. Pham, J. S. Chung, N. T. Khoa, E. J. Kim and S. H. Hahn, *Curr. Appl. Phys.*, 2011, **11**, 805.
78 J. Du, X. Lai, N. Yang, J. Zhai, D. Kisailus, F. Su, D. Wang and L. Jiang, *ACS Nano*, 2011, **5**, 590.
79 K. Maeda and K. Domen, *J. Phys. Chem. C*, 2007, **111**, 7851.
80 M. Miyauchi, A. Nakajima, T. Watanabe and K. Hashimoto, *Chem. Mater.*, 2002, **14**, 2812.
81 B. Li and H. Cao, *J. Mater. Chem.*, 2011, **21**, 3346.
82 T. Xu, L. Zhang, H. Cheng and Y. Zhu, *Appl. Catal., B*, 2011, **101**, 382.
83 H. Sun, L. Cao and L. Lu, *Nano Res.*, 2011, **4**, 550.
84 H. Hu, X. Wang, F. Liu, J. Wang and C. Xu, *Synth. Met.*, 2011, **161**, 404.
85 Q. Li, B. Guo, J. Yu, J. Ran, B. Zhang, H. Yan and J. Gong, *J. Am. Chem. Soc.*, 2011, **133**, 10878.
86 R. Abea, *J. Photochem. Photobiol., C*, 2010, **11**, 179.
87 L. Zhang, H. Wang, Z. Chen, P. K. Wong and J. Liu, *Appl. Catal. B: Environ*, 2011, **106**, 1.
88 E. Gao, W. Wang, M. Shang and J. Xu, *Phys. Chem. Chem. Phys.*, 2011, **13**, 2887.
89 Y. Ng, A. Iwase, A. Kudo and R. Amal, *J. Phys. Chem. Lett.*, 2010, **1**, 2607.
90 F. Zhou, R. Shi and Y. Zhu, *J. Mol. Catal. A: Chem.*, 2011, **340**, 77.
91 Y. Fu and X. Wang, *Ind. Eng. Chem. Res.*, 2011, **50**, 7210.
92 X. Zhang, X. Quan, S. Chen and H. Yu, *Appl. Catal., B*, 2011, **105**, 237.
93 M. Zhu, P. Chen and M. Liu, *ACS Nano*, 2011, **5**, 4529.
94 L. Zhang, Z. Xiong and X. S. Zhao, *ACS Nano*, 2010, **4**, 7030.
95 Z. Xiong, L. Zhang and X. Zhao, *Chem. Eur. J.*, 2011, **17**, 2428.
96 G. Palmisano, E. Garcia-Lopez, G. Marcı, V. Loddo, S. Yurdakal, V. Augugliaro and L. Palmisano, *Chem. Commun.*, 2010, **46**, 7074.
97 G. Palmisano, V. Augugliaro, M. Pagliaro and L. Palmisano, *Chem. Commun.*, 2007, 3425.
98 G. Li, D. Zhang, J. C. Yu and M. Leung, *Environ. Sci. Technol.*, 2010, **44**, 4276.
99 F. L. Fu, H. Y. Zeng, Q. H. Cai, R. L. Qiu, J. Yu and Y. Xiong, *Chemosphere*, 2007, **69**, 1783.
100 S. C. Roy, O. K. Varghese, M. Paulose and C. A. Grimes, *ACS Nano*, 2010, **4**, 1259.
101 S. Yan, L. Wan, Z. Li and Z. Zou, *Chem. Commun.*, 2011, **47**, 5632.
102 A. R. Khataee and M. B. Kasiri, *J. Mol. Catal. A: Chem.*, 2010, **328**, 8.
103 W. Zhang, L. Zou and L. Wang, *Appl. Catal., A*, 2009, **371**, 1.
104 J. Liu, Z. Wang, L. Liu and W. Chen, *Phys. Chem. Chem. Phys.*, 2011, **13**, 13216.
105 P. Wang, Y. Zhai, D. Wang and S. Dong, *Nanoscale*, 2011, **3**, 1640.
106 Z. Xiong, L. Zhang, J. Ma and X. S. Zhao, *Chem. Commun.*, 2010, **46**, 6099.
107 Y. H. Ng, I. V. Lightcap, K. Goodwin, M. Matsumura and P. V. Kamat, *J. Phys. Chem. Lett.*, 2010, **1**, 2222.
108 T. Nguyen-Phan, V. Pham, E. Shin, H. Pham, S. Kim, J. Chung, E. Kim and S. Hur, *Chem. Eng. J.*, 2011, **170**, 226.
109 B. Neppolian, A. Bruno, C. L. Bianchi and M. Ashokkumar, *Ultrason. Sonochem.*, 2012, **19**, 9.
110 Z. Liu, J. T. Robinson, X. M. Sun and H. J. Dai, *J. Am. Chem. Soc.*, 2008, **130**, 10876.
111 S. Sakthivel and H. Kisch, *Angew. Chem., Int. Ed.*, 2003, **42**, 4908.
112 X. Wang, L. J Zhi and K. Mullen, *Nano Lett.*, 2008, **8**, 323.
113 K. Manga, Y. Zhou, Y. Yan and K. Loh, *Adv. Funct. Mater.*, 2009, **19**, 3638.
114 J. Zhu and M. Zach, *Curr. Opin. Colloid Interface Sci.*, 2009, **14**, 260.
115 T. Yeh, J. Syu, C. Cheng, T. Chang and H. Teng, *Adv. Funct. Mater.*, 2010, **20**, 2255.
116 J. Shen, M. Shi, B. Yan, H. Ma, N. Li and M. Ye, *Nano Res.*, 2011, **4**, 795.
117 Q. Xiang, J. Yu and M. Jaroniec, *J. Phys. Chem. C*, 2011, **115**, 7355.
118 L. Yuliatiw and H. Yoshida, *Chem. Soc. Rev.*, 2008, **37**, 1592.
119 Y. Liang, B. K. Vijayan, K. A. Gray and M. C. Hersam, *Nano Lett.*, 2011, **11**, 2865.
120 G. Jiang, Z. Lin, C. Chen, L. Zhu, Q. Chang, N. Wang, W. Wei and H. Tang, *Carbon*, 2011, **49**, 2693.
121 O. Akhavan and E. Ghaderi, *J. Phys. Chem. C*, 2009, **113**, 20214.
122 B. Li, X. Zhang, X. Li, L. Wang, R. Han, B. Liu, W. Zheng, X. Li and Y. Liu, *Chem. Commun.*, 2010, **46**, 3499.
123 L. Zhang, S. Diao, Y. Nie, K. Yan, N. Liu, B. Dai, Q. Xie, A. Reina, J. Kong and Z. Liu, *J. Am. Chem. Soc.*, 2011, **133**, 2706.
124 I. V. Lightcap, T. H. Kosel and P. V. Kamat, *Nano Lett.*, 2010, **10**, 577.
125 S. Ding, J. Chen, D. Luan, F. Y. C. Boey, S. Madhavibc and X. W. Lou, *Chem. Commun.*, 2011, **47**, 5780.
126 J. Liu, L. Liu, H. Bai, Y. Wang and D. Sun, *Appl. Catal., B*, 2011, **106**, 76.
127 A. Mukherji, B. Seger, G. Q. Lu and L. Wang, *ACS Nano*, 2011, **5**, 3483.
128 D. Wang, D. Choi, J. Li, Z. Yang, Z. Nie, R. Kou, D. Hu, C. Wang, L. V. Saraf, J. Zhang, I. A. Aksay and J. Liu, *ACS Nano*, 2009, **3**, 907.
129 Y. Qiu, K. Yan, S. Yang, L. Jin, H. Deng and W. Li, *ACS Nano*, 2010, **4**, 6515.
130 N. Li, G. Liu, C. Zhen, F. Li, L. Zhang and H. Cheng, *Adv. Funct. Mater.*, 2011, **21**, 1717.
131 N. J. Bell, Y. H. Ng, A. Du, H. Coster, S. C. Smith and R. Amal, *J. Phys. Chem. C*, 2011, **115**, 6004.
132 A. Du, Y. Ng, N. J. Bell, Z. Zhu, R. Amal and S. C. Smith, *J. Phys. Chem. Lett.*, 2011, **2**, 894.
133 M. F. Craciuna, S. Russob, M. Yamamotoc and S. Taruchac, *Nano Today*, 2011, **6**, 42.
134 D. R. Dreyer, R. S. Ruoff and C. W. Bielawski, *Angew. Chem., Int. Ed.*, 2010, **49**, 9336.
135 V. Singh, D. Joung, L. Zhai, S. Das, S. Khondaker and S. Seal, *Prog. Mater. Sci.*, 2011, **56**, 1178.